Desalination and Water Treatment
www.deswater.com
doi: 10.1080/19443994.2014.963158

56 (2015) 2966–2975
December

Taylor & Francis
Taylor & Francis Group

Dynamic adsorption of methylene blue by melon peel in fixed-bed columns

Chawki Djelloul, Oualid Hamdaoui*

Laboratory of Environmental Engineering, Faculty of Engineering, Department of Process Engineering, Badji Mokhtar—Annaba University, P.O. Box 12, 23000 Annaba, Algeria, Tel./Fax: +213 0 38876560; emails: djelloulchawki@yahoo.fr (C. Djelloul), oualid.hamdaoui@univ-annaba.dz (O. Hamdaoui)

Received 27 February 2014; Accepted 2 September 2014

ABSTRACT

The dynamic adsorption of methylene blue (MB) by melon peel (MP) was studied in packed bed columns. The values of column parameters were predicted as a function of flow rate and initial dye concentration. On evaluating the breakthrough curves, the adsorption isotherms of MB by MP were experimentally determined in batch conditions. The Langmuir model was found to fit the adsorption isotherm data well with a maximum adsorption capacity of 333.33 mg/g at 25°C. A series of column tests using MP as a low-cost adsorbent were performed to determine the breakthrough curves with varying initial dye concentrations and flow rates. High bed height, low flow rate and high initial dye concentration were found to be the better conditions for maximum dye adsorption. To predict the breakthrough curves and to determine the characteristic parameters of the column useful for process design, four kinetic models namely Bohart and Adams, Clark, Wolborska, and Yoon and Nelson were applied to experimental data. All models were found suitable for describing the whole, or a definite part of the dynamic behavior of the column, with respect to flow rate and initial dye concentration. The initial segment of the breakthrough curve was not well fitted by the Wolborska model, while the whole breakthrough curve was well predicted by the Bohart and Adams, Clark, and the Yoon and Nelson models. The findings revealed that MP has a high adsorption potential, and it could be used to treat dye-containing effluents.

Keywords: Methylene blue; Dynamic adsorption; Fixed bed; Melon peel; Modeling

1. Introduction

Dyes usually have a synthetic origin and complex aromatic molecular structures that possibly come from coal-tar based hydrocarbons such as benzene, naphthalene, anthracene, toluene, and xylene. Today, there are more than 10,000 dyes available commercially [1]. Increased use of dyes in the textile, paper, rubber, plastics, cosmetics, pharmaceutical, and food industries often poses pollution problems in the form of colored wastewater that is discharged into water bodies. Even small quantities of dyes can color large water bodies, which not only affects asthetic merit but also reduces sunlight penetration and photosynthesis. In addition, some dyes or their metabolites are toxic, mutagenic, or carcinogenic [2,3]. Dyes are recalcitrant molecules that are difficult to degrade biologically.

The removal of color from dye-bearing effluents is a major problem due to the difficulty in treating such wastewaters by conventional treatment methods.

*Corresponding author.

Furthermore, these processes are costly and cannot effectively be used to treat the wide range of dye wastewater. Among the various treatment processes, adsorption is one of the effective and attractive processes to remove dyes, and also to control chemical and biochemical oxygen demands [4,5].

Several adsorbents are eligible for such a purpose. Activated carbon (powdered or granular) is the most widely used adsorbent, because it has excellent adsorption efficiency for organic compounds. However, activated carbon is considered as an expensive adsorbent, which makes the wastewater treatment as a prohibitive and costly step. Several studies have tried to replace the activated carbon with less expensive materials. Therefore, there is growing interest in using low-cost, easily-available materials, for the adsorption of dye colors. Consequently, a number of low cost, easily-available materials are being studied for the removal of different dyes from aqueous solutions at different operating conditions [6–25].

Methylene blue (MB) is selected as a model compound, in order to evaluate the capacity of adsorbents for the removal of dye from aqueous solutions. MB dye has wider applications that include coloring paper, temporary hair colorants, dyeing cottons and wools, and coating for paper stock, etc. Melon peel (MP) was selected for its abundance, availability, and/or economical relevance. MP is capable of removing MB and can be considered as an efficient and low-cost adsorbent for dyes [26]. Our previous study [26] has been conducted in batch mode, which is usually limited to the treatment of small quantities of wastewater. The adsorption capacity parameter obtained from a batch experiment is useful in providing information about the effectiveness of adsorbate–adsorbent system [27]. However, the data obtained under batch conditions are generally not applicable to most treatment systems (such as column operations) where contact time is not sufficiently long for the attainment of equilibrium [27]. Hence, there is a need to perform equilibrium studies using columns. Additionally, no work has been regarded for the adsorption of MB by MP in continuous mode using fixed-bed columns. From the perspective of process modeling, the dynamic behavior of a fixed-bed column is described in terms of the effluent concentration–time profile, i.e. the breakthrough curve. The purpose of the present paper is to study and model the removal of MB from aqueous solutions by adsorption onto MP in fixed-bed columns.

2. Materials and methods

2.1. Adsorbate and adsorbent

The cationic dye, MB ($C_{16}H_{18}N_3SCl$), was obtained from Sigma–Aldrich with analytical grade, that was used without further purification. Required amount of dye was dissolved in distilled water to prepare 1,000 mg/L stock solution that was later diluted to required concentrations.

MP was collected in summer from the region of Annaba (Algeria). It was dried at ambient air hangs for 2–3 days, and then it was ground and sieved using a vibrating sieve (diameter between 0.5 and 1 mm). The obtained material was washed several times with distilled water until the color of the wash water disappeared. The MP was then dried at 50°C in an oven for 12 h, and then cooled in a desiccator and packaged in sealed bottles.

2.2. Scanning electron microscopy and Fourier transform

Scanning electron microscopy (SEM) analysis was carried out on the MP to study its surface texture. Fourier transform infrared (FTIR) analysis was applied on the MP to determine the surface functional groups, by using FTIR spectroscope (FTIR-2000, Perkin–Elmer), where the spectra were recorded from 4,000 to 400 cm^{-1}.

2.3. Adsorption isotherms

Adsorption equilibrium experiments were carried out by adding a fixed amount of MP (0.4 g), into a number of sealed glass flasks containing a definite volume (200 mL in each case), of different initial concentrations (25–500 mg/L) of MB solution without changing their pH. The flasks were then placed in a thermostatic water bath in order to maintain a constant temperature (25°C), and stirring was provided at 300 rpm to ensure equilibrium was reached. Samples of solutions were analyzed for the remaining dye concentration.

The amount of MB uptake by the adsorbent, q_e (mg/g), was obtained as follows

$$q_e = \frac{(C_0 - C_e) \times V}{W} \quad (1)$$

where C_0 and C_e (mg/L) are the liquid-phase concentrations of MB at initial time and equilibrium time, respectively, V (L) is the volume of the solution, and W (g) is the mass of used adsorbent.

2.4. Adsorption in continuous flow column

In fixed-bed columns, the solute concentration in the effluent is free of the target solute until breakthrough of solute occurs. On that account, the behavior of MP in a fixed-bed column operation at a constant temperature (25°C) was studied to determine the breakthrough point that will lead to the column scale-up approach. A glass column (1 cm in diameter) was packed with a fixed-bed height (10 cm) of adsorbent on a glass–wool support and was loaded with 50 or 25 mg/L of MB solution. The working pH was that of the solution and was not controlled. Fixed-bed up-flow adsorber, used in order to avoid preferential paths and no-flow zones, was fed by a peristaltic pump at a constant flow rate, ranging from 0.6 to 1.3 L/h. Interconnecting tubing and fittings are made of polytetrafluoroethylene (PTFE). Effluent samples were analyzed to yield output concentration breakthrough curves.

The breakthrough time (the time at which dye concentration in the effluent reached 3% of the initial concentration) and bed exhaustion time (the time at which dye concentration in the effluent reached influent concentration) were used to evaluate the breakthrough curves.

3. Results and discussion

3.1. SEM and FTIR of MP

Fig. 1(a) and (b) shows the SEM micrographs of MP. It is clear that MP has a rough surface with heterogeneous pores and cavities. This indicates that there is a good possibility for MB dye to get trapped and adsorbed.

The FTIR spectrum obtained (Fig. 2) for the MP displayed the following bands: 3,411.07 cm^{-1}: O–H stretch; 2,919.01 cm^{-1}: C–H stretch; 2,130.00 cm^{-1}: C=N stretch; 1,736.82: C=O stretch; 1,635.25 cm^{-1}: C=O stretch; 1,605.00 cm^{-1}: C=C stretch; 1,513.00 cm^{-1}: NH stretch; 1,440.47 cm^{-1}: in-plane –OH bending and C–O stretch; 1,377.64 cm^{-1}: CH_3 deformation; 1,330.21 cm^{-1}: $–NO_2$ aromatic nitro compounds; 1,252.66 cm^{-1}: C–O stretch; 1,160.28 cm^{-1}: C–N stretch; 1,048.00 cm^{-1}: P–O–C strongest band, highest frequencies for aliphatic amines; 667.00: C–O–H twist. It is clear from Fig. 2 that the adsorbent displays a number of absorption peaks, reflecting the complex nature of the adsorbent.

3.2. Isotherm

The adsorption isotherm of MB by MP was determined. A detailed study on the adsorption equilibrium isotherms can be found in a previous paper [26]. The equilibrium adsorption data can be modeled by using different simple models such as Langmuir, Freundlich, and Temkin given, respectively, by the equations:

$$\frac{1}{q_e} = \frac{1}{q_m} + \frac{1}{bq_m} \times \frac{1}{C_e} \tag{2}$$

$$\ln q_e = \ln K_F + \frac{1}{n} \ln C_e \tag{3}$$

$$q_e = \frac{R_g T}{b_t} \ln a_t + \frac{R_g T}{b_t} \ln C_e \tag{4}$$

where q_e is the amount of solute adsorbed per unit weight of the adsorbent at equilibrium (mg/g), C_e is the equilibrium concentration of the solute in the bulk solution (mg/L), q_m is the maximum adsorption capacity (mg/g), b is the constant related to the free energy of adsorption (L/mg), n is a constant indicative of the intensity of the adsorption, K_F is a constant indicative of the relative adsorption capacity of the adsorbent ($mg^{1-\frac{1}{n}} L^{\frac{1}{n}} g^{-1}$), b_t is the Temkin constant related to the heat of adsorption (J/mol), a_t is the Temkin isotherm constant (L/mg), R_g is the gas constant (8.314 J/mol K), and T is the absolute temperature (K).

In order to compare the validity of isotherm equations an average percentage error (APE) is calculated as follows:

$$\text{APE } (\%) = \frac{\sum_{1}^{N} \left| \frac{(q_e)_{\exp} - (q_e)_{cal}}{(q_e)_{\exp}} \right|}{N} \times 100 \tag{5}$$

where the subscripts "exp" and "cal" show the experimental and calculated values, respectively, and N is the number of experimental data.

The values of Langmuir, Freundlich, and Temkin parameters are presented in Table 1. The values of APE and determination coefficients given in Table 1 attest that the adsorption isotherm data could be well simulated by Langmuir isotherm model.

In order to predict the adsorption efficiency of the adsorption process, the dimensionless equilibrium parameter of Hall was determined by using the following equation [28]:

$$R_L = \frac{1}{1 + bC_0} \tag{6}$$

where C_0 is the initial concentration. Values of $R_L < 1$ represent favorable adsorption. The R_L values for MP

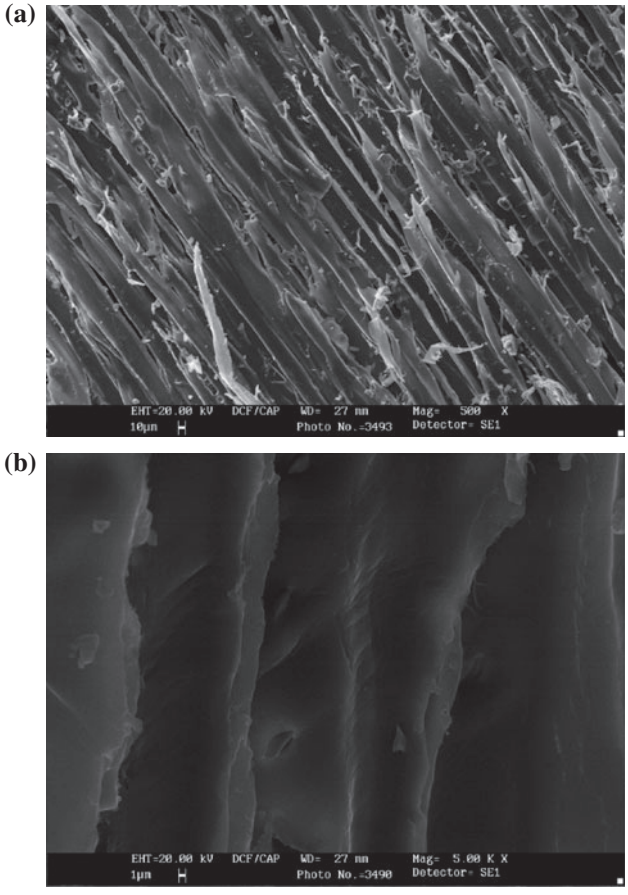

Fig. 1. SEM images for MP: (a) 500×, (b) 5,000×.

are between 0.15 and 0.89 for different temperatures. The obtained R_L values show that our system is favorable.

In general, the values of isotherm constants which were obtained in a batch system show the maximum values of these constants and are considerably higher than those obtained in a fixed bed as flow rate of solution is zero in batch system, that is, the contact time between adsorbate solution and adsorbent approximates infinite. These experimental data are generally used in further studies concerning the dynamic adsorption of solute in column studies for the prediction of breakthrough curves. However, it is important to note that the adsorption isotherms and constants determined in a fixed bed should be used for evaluating the breakthrough curves and kinetic constants to model such a system mathematically.

3.3. Dynamic adsorption

Accumulation of dyes in fixed-bed columns is largely dependent on the initial dye concentration. On the other hand, flow rate is one of the important characteristics in evaluating adsorbents for continuous treatment of dye-laden effluents on an industrial scale. The adsorption breakthrough curves obtained by varying the flow rates (0.6, 0.9 and 1.3 L/h) for different initial MB concentrations (25 and 50 mg L^{-1}) for MP are given in Fig. 3. The breakthrough curves were obtained by plotting the variation of solute concentration in the aqueous solution (normalized with the initial concentration of the dye in the solution) with time. The most efficient adsorption performance will be obtained when the shape of the breakthrough curve is as sharp as possible. Fig. 3 shows that for short times MB in the feed is taken up completely by the column. After a while, dye breakthrough occurs and

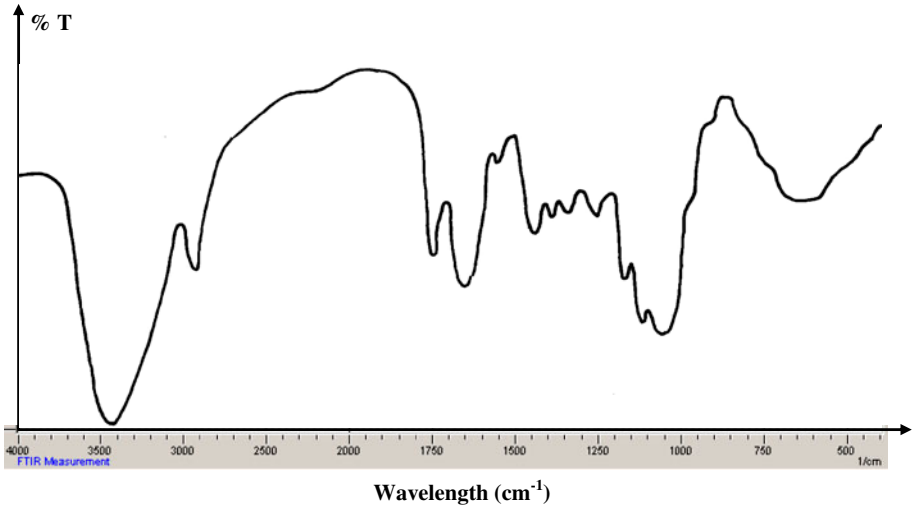

Fig. 2. FTIR spectrum of MP.

Table 1
Langmuir, Freundlich, and Temkin isotherm models constants and determination coefficients for the adsorption of MB by MP at four different temperatures

Model	Parameters			
Langmuir	q_m (mg/g)	b (L/mg) × 10^3	R^2	APE (%)
25℃	333.33	11.3	0.999	5.08
Freundlich	K_F (mg $^{1-1/n}$ $L^{1/n}$ g^{-1})	n	R^2	APE (%)
25℃	6.99	1.51	0.954	16.83
Temkin	a_t (L/mg)	b_t (J/mol)	R^2	APE (%)
25℃	0.29	55.08	0.978	20.67

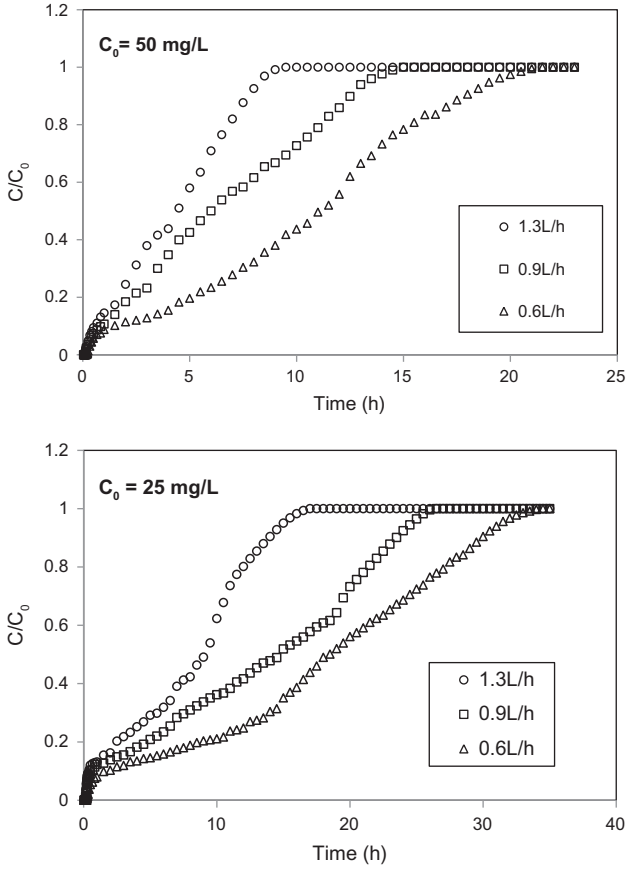

Fig. 3. Breakthrough curves for the adsorption of MB by MP at different initial dye concentrations and flow rates.

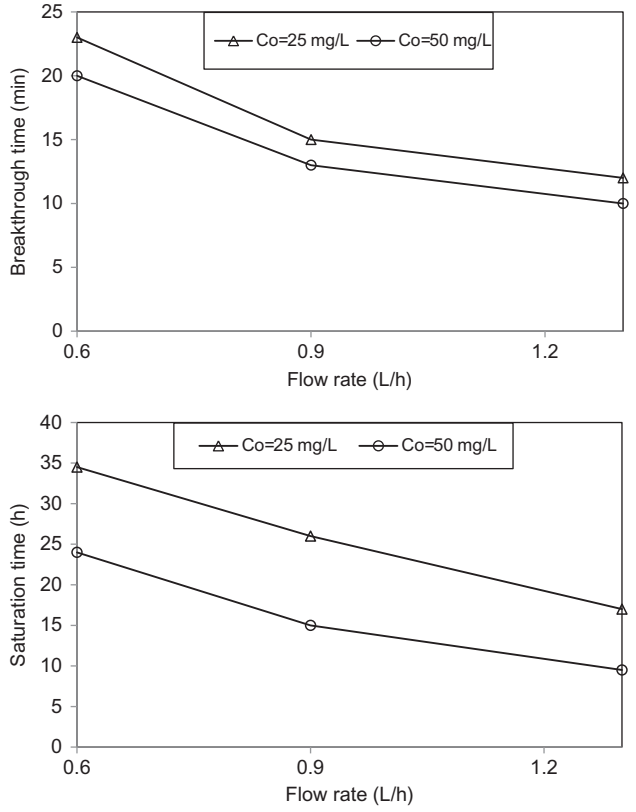

Fig. 4. Variation of breakthrough and saturation times with initial dye concentration and flow rate for MB adsorption by MP.

the effluent concentration increases with time. The breakthrough times were measured when the MB concentration (C) reached 0.03 C_0 (initial concentration). The saturation point is reached when the effluent concentration becomes equal to the feed concentration.

The variation of breakthrough and saturation times with respect to operating variables, influent flow rate and initial dye concentration, is shown in Fig. 4. Both breakthrough and exhaustion times decrease with the increase in the initial dye concentration, as constant binding sites are available for adsorption. The mass of the adsorbent forming the homogenous fixed bed is proportional to the dye adsorbed quantity and as a result, both breakthrough and exhaustion times decrease with the increase in the initial dye concentration. As expected, for a given initial dye concentration, the breakthrough and saturation times are strongly influenced by the flow rate. Fig. 4 shows that by

reducing the flow rate, the breakthrough and exhaustion times increased for a fixed bed height. This flow rate dependence can be accounted for by the fact that for lower value of flow rate, the contact time is longer, and hence the interaction between the dye and the adsorbent is also greater. This leads to higher rate of dye adsorption. On the other hand, for higher flow rate, the contact time is shorter and the dye adsorption is also lower due to lesser interaction.

3.4. Modeling of dynamic adsorption

Successful design of a column adsorption process required prediction of the concentration–time profile or breakthrough curve for the effluent. Various mathematical models can be used to describe fixed-bed adsorption. The dynamic behavior of the column was predicted with the Bohart and Adams, Clark, Wolborska, and Yoon and Nelson models. The breakthrough curves showed the superposition of experimental results (points) and the theoretical calculated points (lines). Linear correlation coefficients (R) showed the fit between experimental data and linearized forms of Bohart and Adams, Clark, Wolborska, and Yoon and Nelson equations.

3.4.1. Application of the Bohart and Adams model

Bohart and Adams [29] established the fundamental equation, describing the relationship between C/C_0 and t for the adsorption of chlorine on charcoal in a fixed-bed column. Although, the original work by Bohart and Adams was done for the gas–charcoal adsorption system, its overall approach can be applied successfully in quantitative description of other systems. This model assumes that the adsorption rate is proportional to both the residual capacity of the activated carbon and the concentration of the sorbing species. The mass transfer rates obey the following equations:

$$\ln\left(\frac{C_0}{C}-1\right)=\frac{K_{BA}N_0Z}{U_0}-K_{BA}C_0t \tag{7}$$

where C is the effluent concentration (mg/L), C_0 the influent concentration (mg/L), K_{BA} the adsorption rate coefficient (L/mg h), N_0 the adsorption capacity (mg/L), Z the bed height (mm), U_0 the linear velocity (mm/h), and t is the time (h).

The model constants K_{BA} and N_0 can be determined from a plot of ln $[(C/C_0)-1]$ against t at a given flow rate, bed height, and initial dye concentration (Fig. 5). The model gave a good fit of the experimental data at all flow rates and all initial dye concentrations

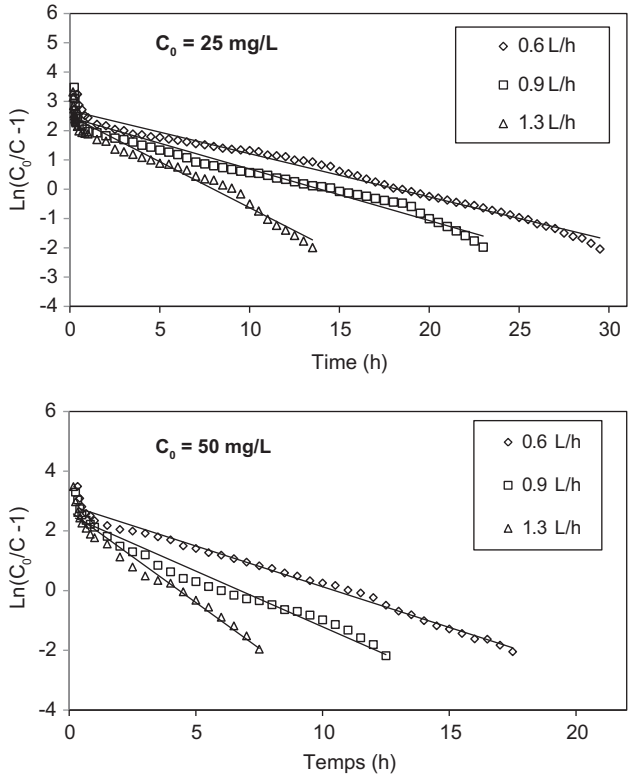

Fig. 5. Bohart and Adams model for dynamic adsorption of MB at various initial dye concentrations and flow rates.

examined with correlation coefficients higher than 0.977. The parameters of Bohart and Adams model are tabulated in Table 2. The value of kinetic constant was influenced by flow rate and increased with increasing flow rate.

3.4.2. Application of the Clark model

The model developed by Clark [30] was based on the use of a mass transfer concept in combination with the Freundlich isotherm:

$$\ln\left[\left(\frac{C_0}{C}\right)^{n-1}-1\right]=\ln A-rt \tag{8}$$

where C is the effluent concentration (mg/L), C_0 the influent concentration (mg/L), n is the Freundlich parameter, and A and r are the Clark constants.

Eq. (8) was applied to the effluent data for the fixed-bed adsorber using linear regression. The Freundlich constant n was used to calculate the parameters in the Clark model. From a plot of ln $[(C_0/C)^{n-1}-1]$ vs. time, the values of r (1/h) and A can be thus determined from its slope, and intercept, respectively (Fig. 6).

Table 2
Bohart and Adams model parameters for MB adsorption by MP at different initial dye concentrations and flow rates

C_0 (mg/L)	Q (L/h)	U_0 (mm/h)	$K_{BA} \times 10^3$ (L/mg h)	N_0 (mg/L)	R
25	0.6	7,639.44	5.88	34,910	0.991
	0.9	11,459.16	7.04	39,928	0.977
	1.3	16,552.11	12.52	33,144	0.980
50	0.6	7,639.44	5.44	40,121	0.993
	0.9	11,459.16	7.46	38,709	0.979
	1.3	16,552.11	12.28	35,989	0.982

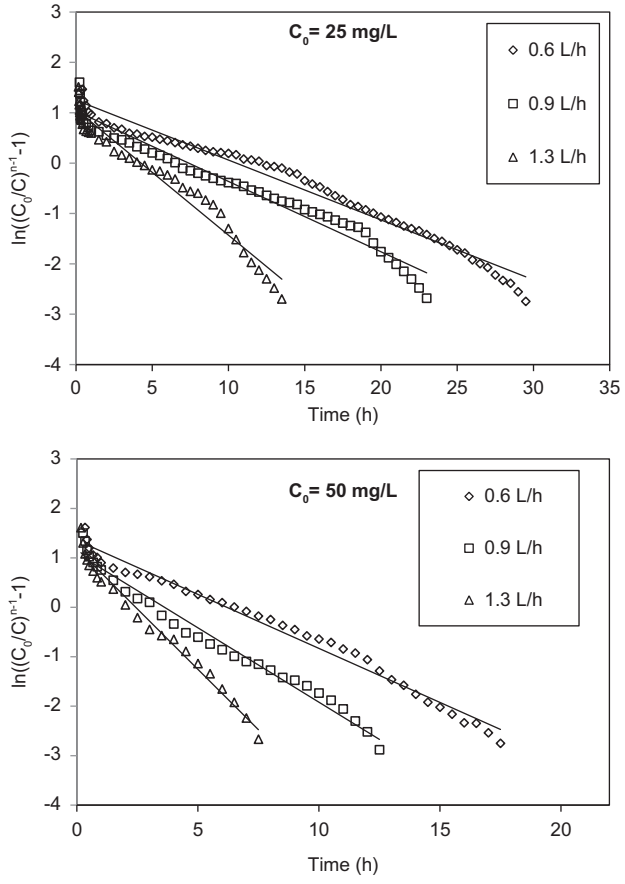

Fig. 6. Clark model for dynamic adsorption of MB at various initial dye concentrations and flow rates.

The parameters of the Clark equation and the correlation coefficients (R) for all flow rates and initial dye concentrations are given in Table 3. It seems that the Clark parameter r decreases with the decrease in flow rate. The correlation coefficients for the linear regression are acceptable showing good agreement of Clark model with the experimental data.

3.4.3. Application of the Wolborska model

Analysis of adsorption-column performance has been attempted by means of the Wolborska model

Table 3
Clark model parameters for MB adsorption by MP at different initial dye concentrations and flow rates

C_0 (mg/L)	Q (L/h)	r (1/h)	ln$A$	R
25	0.6	0.118	1.250	0.987
	0.9	0.139	1.032	0.981
	1.3	0.249	1.062	0.981
50	0.6	0.218	1.355	0.991
	0.9	0.300	1.090	0.989
	1.3	0.488	1.186	0.989

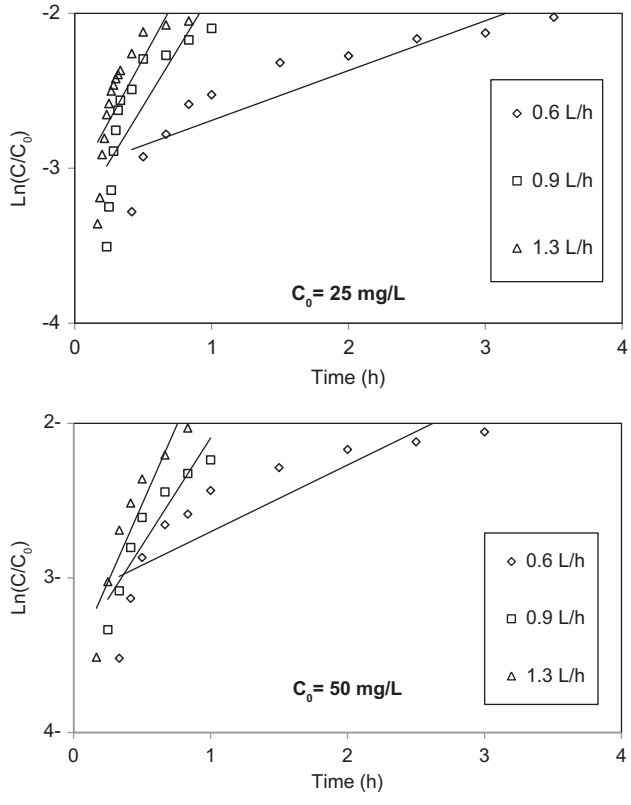

Fig. 7. Wolborska model for dynamic adsorption of MB at various initial dye concentrations and flow rates.

[31] that is used for the description of breakthrough curve in the range of the low concentration. The mass transfer in the fixed-bed adsorption was described by the following equation:

$$\ln\frac{C}{C_0} = \frac{\beta_a C_0}{N_0} t - \frac{\beta_a Z}{U_0} \tag{9}$$

where C is the effluent concentration (mg/L), C_0 the influent concentration (mg/L), β_a is the kinetic coefficient of the external mass transfer (1/h), N_0 is the exchange capacity (mg/L), U_0 is the superficial fluid velocity (mm/h), and Z is the height of the fixed bed (mm).

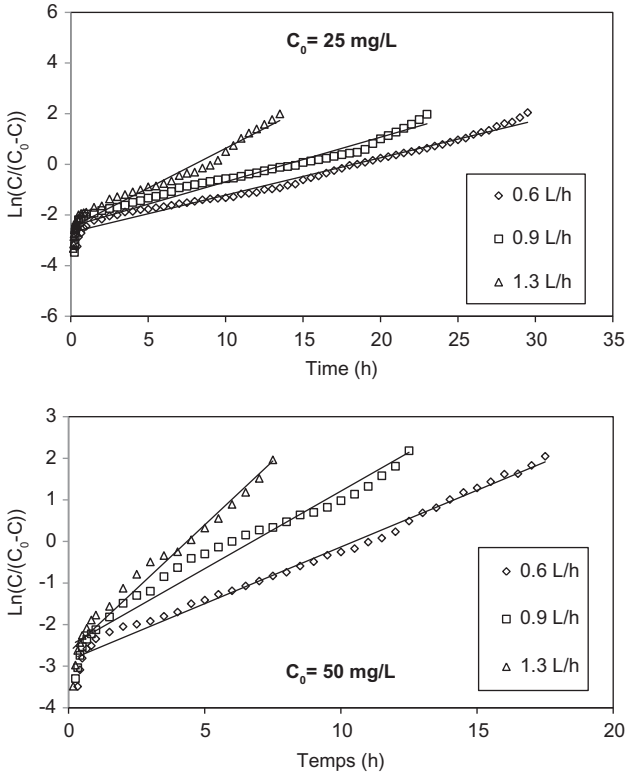

Fig. 8. Yoon and Nelson model for dynamic adsorption of MB at various initial dye concentrations and flow rates.

According to the Wolborska model, the breakthrough curves were linearized by plotting ln C/C_0 vs. t. A nonlinear relationship between ln C/C_0 and t is obtained for ln $C/C_0 < -2$, for all breakthrough curves as shown in Fig. 7. It is clear that the Wolborska model is not valid for the relative concentration region.

3.4.4. Application of the Yoon and Nelson model

Yoon and Nelson [32] developed a relatively simple model addressing the adsorption and breakthrough of adsorbate vapors or gases with respect to activated charcoal. This model was based on the assumption that the rate of decrease in the probability of adsorption for each adsorbate molecule was proportional to the probability of adsorbate adsorption and the probability of adsorbate breakthrough on the adsorbent. The Yoon and Nelson model not only is less complicated than the other models, but also requires no detailed data concerning the characteristics of adsorbate, the type of adsorbent, and the physical properties of adsorption bed.

The Yoon and Nelson equation regarding a single-component system was expressed as:

$$\ln\frac{C}{C_0 - C} = K_{YN} t - t_{1/2} K_{YN} \tag{10}$$

where K_{YN} is the rate constant (1/h), $t_{1/2}$ the time required for 50% adsorbate breakthrough (h), and t is the time (h).

The model developed by Yoon and Nelson was applied to investigate the breakthrough behavior of MB onto a MP. The values of K_{YN} (the rate constant), and $t_{1/2}$ (the time required for 50% adsorbate breakthrough) were determined from ln $[C/(C_0 - C)]$ against t plots at different flow rates and initial dye concentrations (Fig. 8). These values were used to calculate the

Table 4
Yoon and Nelson model parameters for MB adsorption by MP at different initial dye concentrations and flow rates

C_0 (mg/L)	Q (L/h)	K_{YN} (1/h)	$t_{1/2}$ (h) (theoretical)	$t_{1/2}$ (h) (exp.)	R
25	0.6	0.147	18.28	18.5	0.991
	0.9	0.176	13.94	14.68	0.977
	1.3	0.313	8.01	9.09	0.980
50	0.6	0.272	10.50	11.08	0.993
	0.9	0.373	6.76	6	0.979
	1.3	0.614	4.35	4.43	0.982

breakthrough curve. The values of K_{YN} and $t_{1/2}$ are also listed in Table 4. Table 4 indicates that the rate constant K_{YN} increased and the 50% breakthrough time $t_{1/2}$ decreased with increase in both flow rate and initial dye concentration. The data in Table 4 also indicated that $t_{1/2}$ values are in agreement with the experimental results. Similar trend was reported for the adsorption of MB by cedar sawdust and crushed brick [33]. It seems that adsorption breakthrough could be well described by the Yoon and Nelson model.

4. Conclusions

The aim of the present work was to study and model the dynamic removal of MB from aqueous solutions by adsorption onto MP in packed bed columns. The breakthrough curves have been determined at various flow rates and initial dye concentrations at 25˚C. The obtained results showed that both breakthrough and exhaustion times decreased with the increase in the initial dye concentration, as constant binding sites are available for adsorption. The mass of the adsorbent forming the homogenous fixed bed is proportional to the dye-sorbed quantity and as a result both breakthrough and exhaustion times decreased with the increase in the initial dye concentration. For a given initial dye concentration, the lower the flow rate is, the higher are the breakthrough and exhaustion times. This flow rate dependence can be accounted for by the fact that for lower value of flow rate, the contact time is longer and hence the interaction between the dye and the adsorbent is also greater.

The equilibrium distribution of dye between solid and liquid phases was modeled by the Langmuir, Freundlich, and the Temkin isotherm equations. It was found that the equilibrium data were very well described by the Langmuir model.

Several models were applied to experimental data obtained from dynamic studies performed on fixed columns to predict the breakthrough curves and to determine the column kinetic parameters. These models gave good approximations of experimental behavior, with the exception of that of Wolborska, for all flow rates and initial dye concentrations. The initial segment of the breakthrough curve was not well defined by the Wolborska model, while the whole breakthrough curve was well predicted by the Bohart and Adams, Clark, and the Yoon and Nelson models.

This work revealed that MP can be successfully employed as an adsorbent for dye removal from wastewaters.

Acknowledgments

The financial support by the Ministry of Higher Education and Scientific Research of Algeria (project No. J0101120090018) is greatly acknowledged.

Nomenclature

A — constant in the Clark model
b — Langmuir adsorption constant, L/mg
C — effluent MB concentration, mg/L
C_e — non-adsorbed MB concentration at equilibrium, mg/L
C_0 — inlet (feed) or initial MB concentration, mg/L
K_{BA} — kinetic constant in the Bohart and Adams model, L/mg h
K_F — Freundlich adsorption constant, $mg^{1-1/n}\,L^{1/n}\,g^{-1}$
K_{YN} — kinetic constant in the Yoon and Nelson model, L/h
n — Freundlich adsorption constant
N_0 — maximum adsorption capacity, mg/L
q — MB concentration in the solid phase in the column at any time, mg/L
q_e — equilibrium MB uptake per g of adsorbent, mg/g
q_m — maximum adsorption capacity in the Langmuir model, mg/g
Q — flow rate, mL/h
r — constant in the Clark model, 1/h
t — time, h
t_b — time at breakthrough, h
$t_{1/2}$ — time required for 50% adsorbate breakthrough, h
U_0 — superficial velocity, mm/h
V — volume of solution, L
W — weight of adsorbent, g
Z — height of the bed, mm

Greek letter

β_a — kinetic coefficient of the external mass transfer in the Wolborska model, 1/h

References

[1] Ö. Şahin, C. Saka, S. Kutluay, Cold plasma and microwave radiation applications on almond shell surface and its effects on the adsorption of Eriochrome Black T, J. Ind. Eng. Chem. 19 (2013) 1617–1623.
[2] K.C. Chen, J.Y. Wu, C.C. Huang, Y.M. Liang, S.C.J. Hwang, Decolorization of azo dye using PVA-immobilized microorganisms, J. Biotechnol. 101 (2003) 241–252.
[3] G.S. Heiss, B. Gowan, E.R. Dabbs, Cloning of DNA from a *Rhodococcus* strain conferring the ability to decolorize sulfonated azo dyes, FEMS Microbiol. Lett. 99 (1992) 221–226.
[4] G. McKay, M.S. Otterburn, A.G. Sweeney, The removal of colour from effluent using various adsorbents—III. Silica: Rate processes, Water Res. 14 (1980) 15–20.

[5] A. Bhatnagar, A.K. Jain, A comparative adsorption study with different industrial wastes as adsorbents for the removal of cationic dyes from water, J. Colloid Interface Sci. 281 (2005) 49–55.
[6] S.W. Won, S.B. Choi, B.W. Chung, D. Park, J.M. Park, Y.-S. Yun, Biosorptive decolorization of reactive orange 16 using the waste biomass of *Corynebacterium glutamicum*, Ind. Eng. Chem. Res. 43 (2004) 7865–7869.
[7] V.K. Gupta, I. Ali, V.K. Saini, Removal of rhodamine B, fast green, and methylene blue from wastewater using red mud, an aluminum industry waste, Ind. Eng. Chem. Res. 43 (2004) 1740–1747.
[8] V.K. Gupta, I. Ali, V.K. Saini, T. Van Gerven, B. Van der Bruggen, C. Vandecasteele, Removal of dyes from wastewater using bottom ash, Ind. Eng. Chem. Res. 44 (2005) 3655–3664.
[9] C.B. Chandran, D. Singh, P. Nigam, Remediation of textile effluent using agricultural residues, Appl. Biochem. Biotechnol. 102-103 (2002) 207–212.
[10] T. Robinson, B. Chandran, P. Nigam, Removal of dyes from an artificial textile dye effluent by two agricultural waste residues, corncob and barley husk, Environ. Int. 28 (2002) 29–33.
[11] Y.S. Ho, T.H. Chiang, Y.M. Hsueh, Removal of basic dye from aqueous solution using tree fern as a biosorbent, Process. Biochem. 40 (2005) 119–124.
[12] P. Nigam, G. Armour, I.M. Banat, D. Singh, R. Marchant, Physical removal of textile dyes from effluents and solid-state fermentation of dye-adsorbed agricultural residues, Bioresour. Technol. 72 (2000) 219–226.
[13] C. Djelloul, A. Hasseine, Ultrasound-assisted removal of methylene blue from aqueous solution by milk thistle seed, Desalin. Water Treat. 51(28–30) (2013) 5805–5812. doi:10.1080/19443994.2012.760113.
[14] S. Sadaf, H.N. Bhatti, S. Ali, K. Rehman, Removal of Indosol Turquoise FBL dye from aqueous solution by bagasse, a low cost agricultural waste: Batch and column study, Desalin. Water Treat. 52 (2014) 184–198.
[15] E. Khosla, S. Kaur, P.N. Dave, Tea waste as adsorbent for ionic dyes, Desalin. Water Treat. 51 (2013) 6552–6561.
[16] S. Noreen, H.N. Bhatti, S. Nausheen, S. Sadaf, M. Ashfaq, Batch and fixed bed adsorption study for the removal of Drimarine Black CL-B dye from aqueous solution using a lignocellulosic waste: A cost affective adsorbent, Ind. Crop. Prod. 50 (2013) 568–579.
[17] S. Nawaz, H.N. Bhatti, T.H. Bokhari, S. Sadaf, Removal of Novacron Golden Yellow dye from aqueous solutions by low-cost agricultural waste: Batch and fixed bed study, Chem. Ecol. 30 (2014) 52–65.
[18] S. Sadaf, H.N. Bhatti, Batch and fixed bed column studies for the removal of Indosol Yellow BG dye by peanut husk, J. Chin. Inst. Chem. Eng 45 (2014) 541–553.
[19] O. Hamdaoui, Intensification of the sorption of Rhodamine B from aqueous phase by loquat seeds using ultrasound, Desalination 271 (2011) 279–286.
[20] S. Boutemedjet, O. Hamdaoui, Sorption of malachite green by eucalyptus bark as a non-conventional low-cost biosorbent, Desalin. Water Treat. 8 (2009) 201–210.
[21] E.-K. Guechi, O. Hamdaoui, Cattail leaves as a novel biosorbent for the removal of malachite green from liquid phase: Data analysis by non-linear technique, Desalin. Water Treat. 51 (2013) 3371–3380.
[22] M. Zamouche, O. Hamdaoui, A use of cedar cone for the removal of a cationic dye from aqueous solutions by sorption, Energy Procedia 18 (2012) 1047–1058.
[23] M. Zamouche, O. Hamdaoui, Sorption of Rhodamine B by cedar cone: Effect of pH and ionic strength, Energy Procedia 18 (2012) 1228–1239.
[24] O. Hamdaoui, F. Saoudi, M. Chiha, E. Naffrechoux, Sorption of malachite green by a novel sorbent, dead leaves of plane tree: Equilibrium and kinetic modeling, Chem. Eng. J. 143 (2008) 73–84.
[25] O. Hamdaoui, M. Chiha, E. Naffrechoux, Ultrasound-assisted removal of malachite green from aqueous solution by dead pine needles, Ultrason. Sonochem. 15 (2008) 799–807.
[26] C. Djelloul, O. Hamdaoui, Removal of cationic dye from aqueous solution using melon peel as nonconventional low-cost sorbent, Desalin. Water Treat. (2013). doi:10.1080/19443994.2013.833555.
[27] K.S. Bharathi, S.P.T. Ramesh, Fixed-bed column studies on biosorption of crystal violet from aqueous solution by *Citrullus lanatus* rind and *Cyperus rotundus*, Appl. Water Sci. 3 (2013) 673–687.
[28] K.R. Hall, L.C. Eagleton, A. Acrivos, T. Vermeulen, Pore- and solid-diffusion kinetics in fixed-bed adsorption under constant-pattern conditions, Ind. Eng. Chem. Fundam. 5 (1966) 212–223.
[29] G. Bohart, E.N. Adams, Some aspects of the behavior of charcoal with respect to chlorine, J. Am. Chem. Soc. 42 (1920) 523–544.
[30] R.M. Clark, Evaluating the cost and performance of field-scale granular activated carbon systems, Environ. Sci. Technol. 21 (1987) 573–580.
[31] A. Wolborska, Adsorption on activated carbon of p-nitrophenol from aqueous solution, Water Res. 23 (1989) 85–91.
[32] Y.H. Yoon, J.H. Nelson, Application of gas adsorption kinetics I. A theoretical model for respirator cartridge service life, Am. Ind. Hyg. Assoc. J. 45 (1984) 509–516.
[33] O. Hamdaoui, Dynamic sorption of methylene blue by cedar sawdust and crushed brick in fixed bed columns, J. Hazard. Mater. 138 (2006) 293–303.